

**MODELING OF MICROWAVE CIRCUITS EXPLOITING
SPACE DERIVATIVE MAPPING**

M.H. Bakr, J.W. Bandler and N. Georgieva

SOS-98-36-R

November 1998

© M.H. Bakr, J.W. Bandler and N. Georgieva 1998

No part of this document may be copied, translated, transcribed or entered in any form into any machine without written permission. Address inquiries in this regard to Dr. J.W. Bandler. Excerpts may be quoted for scholarly purposes with full acknowledgment of source. This document may not be lent or circulated without this title page and its original cover.

MODELING OF MICROWAVE CIRCUITS EXPLOITING SPACE DERIVATIVE MAPPING

M.H. Bakr, J.W. Bandler and N. Georgieva
Simulation Optimization Systems Research Laboratory
and Department of Electrical and Computer Engineering
McMaster University, Hamilton, Canada L8S 4K1

Tel 905 628 9671
Fax 905 628 1578
Email j.bandler@ieee.org

Abstract

We present a novel approach to microwave circuit modeling, Space Derivative Mapping (SDM). SDM assumes the existence of an empirical model of the structure under consideration. It enables the construction of a space mapping-based locally valid model exploiting, for the first time, both the empirical simulations and the response sensitivity information. Parameter extraction uniqueness is no longer important. The constructed model enjoys higher accuracy than that of linear response approximation. Statistical analysis of waveguide transformers and filters illustrates SDM.

SUMMARY

Introduction

Full-wave simulations of microwave structures are CPU intensive. Developing fast and accurate models for simulating microwave circuits that can be utilized for design purposes over wide ranges of the parameter space is crucial. Space Mapping (SM) was introduced [1, 2] to address this problem.

In this paper we present a novel technique for microwave circuit modeling based on SM. SM assumes the existence of “coarse” and “fine” models for the circuit under consideration. The coarse model is fast but not necessarily very accurate (equivalent circuits, empirical formulas, etc.). The fine model is accurate but CPU intensive. Aggressive Space Mapping (ASM) [2] optimization, for example,

This work was supported in part by the Natural Sciences and Engineering Research Council of Canada under Grants OGP0007239, STP0201832 and through the Micronet Network of Centres of Excellence. N. Georgieva is supported by an NSERC Postdoctorate Fellowship and M.H. Bakr by an Ontario Graduate Scholarship.

J.W. Bandler is also with Bandler Corporation, P.O. Box 8083, Dundas, Ontario, Canada L9H 5E7.

iteratively establishes a mapping between the spaces of the parameters of the two models. After the optimization is completed a matrix \mathbf{B} represents a valid mapping in the vicinity of the optimal design. On the other hand, the originally proposed SM approach [1] establishes a mapping between both spaces by individually extracting a set of coarse model points corresponding to a given set of fine model points as a prerequisite to optimization. The nonuniqueness of any of the extracted coarse model points is likely to result in an inaccurate mapping between the two spaces.

The SDM Modeling (SDMM) technique proposed here creates a locally valid mapping-based model in the vicinity of a point of interest in the fine model space. The technique is based on a novel lemma that estimates the mapping between the two spaces using only a single parameter extraction. The uniqueness of the extracted parameters is not a serious issue. Sensitivity information in both spaces is utilized in the construction of the mapping. The SDMM technique exploits the constructed mapping and coarse model simulations.

Brief Background

We refer to the vector of fine model parameters and the vector of coarse model parameters as \mathbf{x}_{em} and \mathbf{x}_{os} , respectively. The aim of SM optimization is to obtain the set of fine model parameters $\bar{\mathbf{x}}_{em}$ whose fine model response matches the optimal coarse model response evaluated at \mathbf{x}_{os}^* , the optimal coarse model design. The ASM algorithm constructs the mapping iteratively, returning the final design $\bar{\mathbf{x}}_{em}$ and matrix \mathbf{B} representing the mapping at $\bar{\mathbf{x}}_{em}$. A perturbation of $\Delta \mathbf{x}_{em}$ in the fine model space is mapped to a perturbation of $\Delta \mathbf{x}_{os}$ in the coarse model space by [2]

$$\Delta \mathbf{x}_{os} = \mathbf{B} \Delta \mathbf{x}_{em} \quad (1)$$

such that the fine model point $\bar{\mathbf{x}}_{em} + \Delta \mathbf{x}_{em}$ and the coarse model point $\mathbf{x}_{os}^* + \Delta \mathbf{x}_{os}$ have matched responses. The mapping (1) together with the coarse model essentially builds a fast and accurate model for the circuit under consideration in the vicinity of the final design $\bar{\mathbf{x}}_{em}$. It can be used in additional analyses, e.g., statistical analysis.

The New Technique

The SDMM technique is based on the following novel lemma.

Lemma Assume that \mathbf{x}_{os} corresponds to \mathbf{x}_{em} through a parameter extraction process. Then the Jacobian \mathbf{J}_{em} of the fine model responses at \mathbf{x}_{em} and the Jacobian \mathbf{J}_{os} of the coarse model responses at \mathbf{x}_{os} are related by

$$\mathbf{J}_{em} = \mathbf{J}_{os} \mathbf{B} \quad (2)$$

where \mathbf{B} is a valid mapping between the two spaces at \mathbf{x}_{os} and \mathbf{x}_{em} .

The proof of this novel lemma is omitted here for the sake of brevity.

It follows from (2) that

$$\mathbf{B} = \left(\mathbf{J}_{os}^T \mathbf{J}_{os} \right)^{-1} \mathbf{J}_{os}^T \mathbf{J}_{em} \quad (3)$$

Relation (3) assumes that \mathbf{J}_{os} is a full rank matrix and $m \geq n$, where n is the number of parameters and m is the number of responses. It shows that \mathbf{B} can be obtained by multiplying the Jacobian of the fine model responses with the pseudoinverse of \mathbf{J}_{os} . A similar formula can be obtained using singular value decomposition [3] if \mathbf{J}_{os} is not full rank.

Suppose it is required to obtain a fast and accurate approximation to the fine model response in the vicinity of a particular point \mathbf{x}_{em}^* . We denote by \mathbf{J}_{em}^* the Jacobian of the fine model responses at \mathbf{x}_{em}^* . The first step is to obtain the point $\bar{\mathbf{x}}_{os}$ corresponding to \mathbf{x}_{em}^* through the parameter extraction problem

$$\bar{\mathbf{x}}_{os} = \arg \left\{ \min_{\mathbf{x}_{os}} \left\| \mathbf{R}_{em}(\mathbf{x}_{em}^*) - \mathbf{R}_{os}(\mathbf{x}_{os}) \right\| \right\} \quad (4)$$

The Jacobian $\bar{\mathbf{J}}_{os}$ of the coarse model responses at $\bar{\mathbf{x}}_{os}$ may be estimated by perturbation. Both the parameter extraction step (4) and the evaluation of the Jacobian of the coarse model responses should add no significant overhead since the coarse model is assumed to be much faster than the fine model. The matrix \mathbf{B} is then calculated by applying (3) as

$$\mathbf{B} = \left(\bar{\mathbf{J}}_{os}^T \bar{\mathbf{J}}_{os} \right)^{-1} \bar{\mathbf{J}}_{os}^T \mathbf{J}_{em}^* \quad (5)$$

Once \mathbf{B} is available the SDM model is provided by the simple formula

$$\mathbf{R}_{em}(\mathbf{x}_{em}) \approx \mathbf{R}_{os}(\bar{\mathbf{x}}_{os} + \mathbf{B}(\mathbf{x}_{em} - \mathbf{x}_{em}^*)) \quad (6)$$

This model is expected to enjoy a wide region of validity as the two models are assumed to share the same physical structure. The similarity in the nonlinear behavior of the two models makes this model superior to linear response approximation in the fine model space.

The uniqueness of the parameter extraction problem (4) should not affect the SDM model. If a different extracted point $\bar{\mathbf{x}}_{os}$ is obtained, a different mapping \mathbf{B} given by (5) will be a valid mapping at the two points \mathbf{x}_{em}^* and $\bar{\mathbf{x}}_{os}$. The SDM model given by (6) is still an accurate model.

Two-Section Waveguide Transformer

The SDMM technique is tested on the statistical analysis of a two-section waveguide transformer [4] shown in Fig. 1. The coarse model is an “ideal” analytical model which neglects the junction discontinuity effects while the fine model is a more accurate “nonideal” analytical model which includes the junction discontinuity effects [4]. The design constraints for this problem are

$$v_{swr} \leq 1.04 \text{ for } 5.8 \text{ GHz} \leq f \leq 6.6 \text{ GHz} \quad (7)$$

Optimizable parameters are the height and the length of each waveguide section.

The fine model is optimized using the minimax optimizer available in OSA90/hope [5]. The optimal fine model design is shown in the second column of Table I.

An estimate for the Jacobian of the fine model responses is obtained. Parameter extraction is applied to get $\bar{\mathbf{x}}_{os}$. See the third column of Table I. Fig. 2. shows the optimal fine model response and the coarse model response at $\bar{\mathbf{x}}_{os}$. The Jacobian $\bar{\mathbf{J}}_{os}$ is estimated using perturbation. An estimate for \mathbf{B} is calculated using (5) as

$$\mathbf{B} = \begin{bmatrix} 0.4066 & -0.0196 & 0.0002 & 0.0092 \\ -1.1897 & 1.0023 & -0.0129 & 0.0325 \\ -0.5057 & -0.0838 & 0.4234 & 0.6903 \\ 0.0161 & 0.0861 & 0.5288 & 0.4015 \end{bmatrix} \quad (8)$$

The designable parameters are assumed to be uniformly distributed with equal relative tolerances. We apply SDMM to carry out space-mapped statistical analysis using (6) with 100 samples. Tolerances considered are 1%, 2% and 4%. The corresponding yield estimates are given in the second column of Table II. We verified the accuracy of the estimates by carrying out a statistical analysis using fine model simulations. The corresponding yield estimates are given in the third column of Table II. The SDM yield estimates agree well with fine model yield estimates. Corresponding responses are shown in Figs. 3, 4 and 5.

Three-section Rounded Edge Waveguide Transformer [6]

The designable parameters for this problem are the height and length of each waveguide section. The specifications are $|S_{11}| \leq -30$ dB for the range 9.5 GHz to 15 GHz. The fine model of this circuit exploits HP HFSS [7] through HP Empire3D [6]. The coarse model exploits an ideal empirical model that does not take into account the rounding of the corners. One quadrant of the transformer is shown in Fig. 6. We exploit geometrical symmetry to reduce the required CPU time of HP HFSS.

The minimax optimizer available in HP Empire3D is applied to the design of the transformer. The optimal fine model design is shown in the second column of Table III. The corresponding point $\bar{\mathbf{x}}_{os}$, obtained through parameter extraction, is given in the third column of Table III. The optimal fine model response and the coarse model response at $\bar{\mathbf{x}}_{os}$ are shown in Fig. 7.

An estimate for \mathbf{J}_{em}^* is obtained by linear approximation [8] using the database already generated during direct optimization of the transformer. A simple MATLAB program [9] is coded to determine the base points needed. Microsoft Excel [10] processes the database and extracts the fine model responses at the base points. $\bar{\mathbf{J}}_{os}$ is estimated using perturbation. An estimate for \mathbf{B} is calculated using (5) as

$$\mathbf{B} = \begin{bmatrix} 1.60380 & -0.63084 & -1.95487 & 0.25696 & -0.19372 & 0.05510 \\ 0.84904 & 0.44277 & -0.62860 & 0.38383 & -0.27637 & 0.20849 \\ 0.37935 & -0.12923 & -0.11940 & 0.25799 & -0.19919 & 0.13550 \\ -2.39260 & 2.26734 & 1.47112 & 0.04667 & -0.88791 & -0.11676 \\ -0.01317 & -0.35376 & -0.09695 & 0.10135 & 0.99794 & 0.36326 \\ 0.68861 & -0.31207 & 0.16520 & 0.39093 & 0.29544 & 0.37047 \end{bmatrix} \quad (9)$$

Figs. 8-10 compare statistically generated responses obtained using 100 random points, uniformly distributed with 0.5%, 2% and 4% relative tolerances.

Figs. 11-13 compare the accuracy of this SDM model with linear approximation in the fine model space. These figures show the absolute values of the errors between the fine model responses (the reflection coefficients) and those predicted by SDM and linear approximation. For small tolerances such as 0.5% the two models are comparable. For larger tolerances, the SDM model shows much higher accuracy than that of linear approximation.

A Six-Section H-Plane Waveguide Filter [11, 12]

The design specifications are

$$|S_{11}| \leq 0.16 \quad \text{for } 5.4 \text{ GHz} \leq f \leq 9.0 \text{ GHz} \quad (10)$$

$$|S_{11}| \geq 0.85 \quad \text{for } f \leq 5.2 \text{ GHz} \quad \text{and} \quad |S_{11}| \geq 0.5 \quad \text{for } 9.5 \text{ GHz} \leq f \quad (11)$$

A waveguide with a cross-section of 1.372 inches by 0.622 inches (3.485 cm by 1.58 cm) is used. As shown in Fig. 14, the six sections are separated by seven H-plane septa, which have a finite thickness of 0.02 inches (0.508 mm).

Optimizable parameters are the four septa widths W_1 , W_2 , W_3 and W_4 and the three resonator lengths L_1 , L_2 and L_3 . The coarse model (Fig. 15) consists of lumped inductances and dispersive transmission line sections simulated by OSA90/hope [5]. For the equivalent inductances of the H-plane septa we utilize formulas by Marcuvitz [13]. The fine model exploits HP HFSS [7] through HP Empipe3D [6].

The point \mathbf{x}_{em}^* is given in the second column of Table IV. The extracted $\bar{\mathbf{x}}_{os}$ is given in the third column of Table IV. The corresponding responses are shown in Fig. 16.

An estimate of \mathbf{J}_{em}^* is calculated similarly to the previous example. $\bar{\mathbf{J}}_{os}$ is estimated by perturbation. Using (5) the mapping is given by

$$\mathbf{B} = \begin{bmatrix} 0.97720 & -0.01442 & -0.01947 & -0.06367 & -0.82207 & -0.03473 & -0.00852 \\ 0.00783 & 0.90185 & -0.00161 & -0.01033 & -1.11069 & 0.27349 & 0.15620 \\ -0.00193 & 0.19867 & 0.85915 & -0.01096 & -0.60203 & -0.15445 & -0.11624 \\ -0.07231 & 0.01827 & -0.01416 & 0.94934 & -0.64212 & -0.00438 & -0.08671 \\ -0.03969 & -0.06505 & -0.02930 & 0.00021 & 1.16453 & -0.03594 & -0.09786 \\ -0.03040 & 0.07777 & -0.07685 & 0.03166 & 0.01267 & 0.98957 & 0.01766 \\ -0.00115 & -0.02554 & 0.048959 & -0.02949 & -0.13667 & -0.01311 & 1.00263 \end{bmatrix} \quad (12)$$

Figs. 17-19 compare statistically generated responses obtained using 100 random points, uniformly distributed with 1%, 4% and 8% relative tolerances.

Figs. 20-22 compare the accuracy of this SDM model with linear approximation in the fine model space. For small tolerances such as 1% the two models are comparable. For larger tolerances, the SDM model shows much higher accuracy than that of linear approximation.

Conclusions

We present a novel technique for the fast and accurate modeling of microwave circuits. The technique exploits a Space Derivative Mapping (SDM) approach in the construction of a space-mapping based model. We introduce a novel lemma that enables the establishment of the mapping between the designable input parameters to an electromagnetic optimizer and the parameters of a corresponding empirical model with no additional overhead of electromagnetic simulations. SDM modeling (SDMM) alleviates the extraction uniqueness problem involved in prior SM algorithms and the necessity of applying SM optimization in the ASM algorithm. The SDM model is demonstrated to enjoy a wider range of validity than that of linear response approximation. Statistical analysis of microwave circuits exemplifies our technique.

References

- [1] J.W. Bandler, R.M. Biernacki, S.H. Chen, P.A. Grobelny and R.H. Hemmers, "Space mapping technique for electromagnetic optimization," *IEEE Trans. Microwave Theory Tech.*, vol. 42, 1994, pp. 2536-2544
- [2] J.W. Bandler, R.M. Biernacki, S.H. Chen, R.H. Hemmers and K. Madsen, "Electromagnetic optimization exploiting aggressive space mapping," *IEEE Trans. Microwave Theory Tech.*, vol. 43, 1995, pp. 2874-2882.
- [3] P.E. Gill, W. Murray and M.H. Wright, *Numerical Linear Algebra and Optimization*. New York: Addison Wesley, First Edition, 1991.
- [4] J.W. Bandler, "Computer optimization of inhomogeneous waveguide transformers," *IEEE Trans. Microwave Theory Tech.*, vol. MTT-17, 1969, pp. 563-571.
- [5] *OSA90/hope™* Version 4.0, formerly Optimization Systems Associates Inc., P.O. Box 8083, Dundas, ON, Canada, L9H 5E7, 1997, now HP EEsof Division, 1400 Fountaingrove Parkway, Santa Rosa, CA 95403-1799.
- [6] *HP Empipe3D™* Version 5.2, HP EEsof Division, 1400 Fountaingrove Parkway, Santa Rosa, CA 95403-1799, 1998.
- [7] *HP HFSS™* Version 5.2, HP EEsof Division, 1400 Fountaingrove Parkway, Santa Rosa, CA 95403-1799, 1998.
- [8] J.W. Bandler, R.M. Biernacki, S.H. Chen, L.W. Hendrick and D. Omeragic, "Electromagnetic optimization of 3-D structures," *IEEE Trans. Microwave Theory Tech.*, vol. 45, 1997, pp.770-779.
- [9] *MATLAB®* Version 5.0, The Math. Works, Inc., 24 Prime Park Way, Natick, MA 01760, 1997.
- [10] *Microsoft® Excel 97*, Microsoft Corporation, 1997.
- [11] L. Young and B.M. Schiffman, "A useful high-pass filter design," *Microwave J.*, vol. 6, 1963, pp. 78-80.
- [12] G.L. Matthaei, L. Young and E.M. Jones, *Microwave Filters, Impedance-Matching Network and Coupling Structures*. New York: McGraw-Hill, First Edition, 1964.
- [13] N. Marcuvitz, *Waveguide Handbook*. New York: McGraw-Hill, First Edition, 1951, pp. 221.

TABLE I
 THE OPTIMAL FINE MODEL DESIGN AND THE CORRESPONDING
 EXTRACTED COARSE MODEL POINT FOR THE TWO-SECTION
 WAVEGUIDE TRANSFORMER

Parameter	\mathbf{x}_{em}^*	$\bar{\mathbf{x}}_{os}$
b_1	0.71737	0.71468
b_2	1.39574	1.39092
L_1	1.55077	1.64691
L_2	1.50654	1.59799

all values are in cm

TABLE II
 THE YIELD FOR THE TWO-SECTION WAVEGUIDE TRANSFORMER OBTAINED USING THE
 SDM STATISTICAL ANALYSIS COMPARED WITH FINE MODEL YIELD

Tolerance	Space-Mapped Yield	Fine Model Yield
1.0%	59%	53%
2.0%	27%	19%
4.0%	8%	3%

TABLE III
 THE OPTIMAL FINE MODEL DESIGN AND THE CORRESPONDING
 EXTRACTED COARSE MODEL POINT FOR THE THREE-SECTION
 WAVEGUIDE TRANSFORMER WITH ROUNDED CORNERS

Parameter	\mathbf{x}_{em}^*	$\bar{\mathbf{x}}_{os}$
L_1	0.32408	0.32507
L_2	0.32492	0.32747
L_3	0.33114	0.33223
h_1	0.20750	0.21543
h_2	0.26025	0.27415
h_3	0.32815	0.33700
All values are in inches		

TABLE IV
 THE OPTIMAL FINE MODEL DESIGN AND THE CORRESPONDING
 EXTRACTED COARSE MODEL POINT FOR THE SIX-SECTION
 WAVEGUIDE FILTER

Parameter	\mathbf{x}_{em}^*	$\bar{\mathbf{x}}_{os}$
C_1	0.51336	0.49956
C_2	0.47293	0.45926
C_3	0.45031	0.43709
C_4	0.44575	0.43274
L_1	0.63570	0.65468
L_2	0.63910	0.65873
L_3	0.65681	0.67579
All values are in inches		

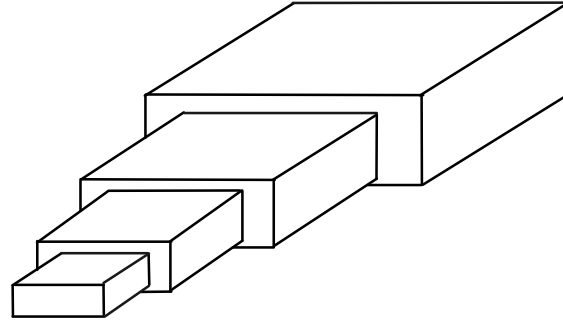


Fig. 1. The two-section waveguide transformer.

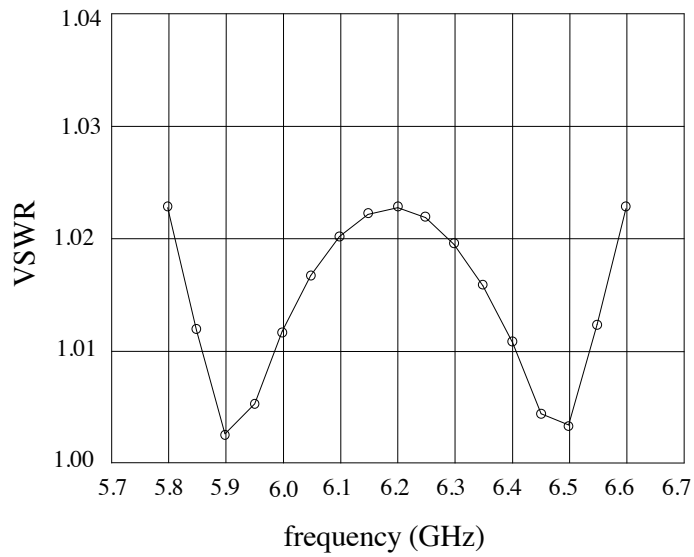
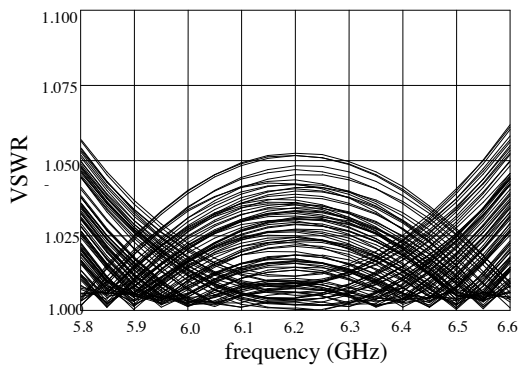
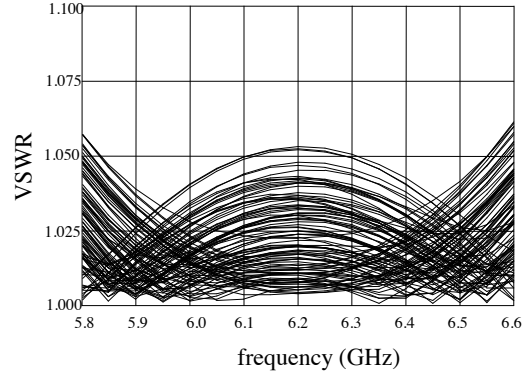


Fig. 2. The optimal fine model response (o) and the response (—) at the corresponding coarse model point for the two-section waveguide transformer.

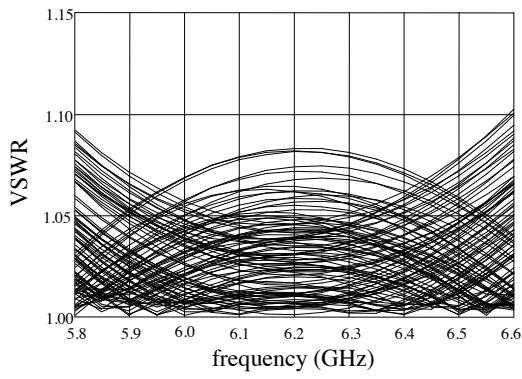


(a)

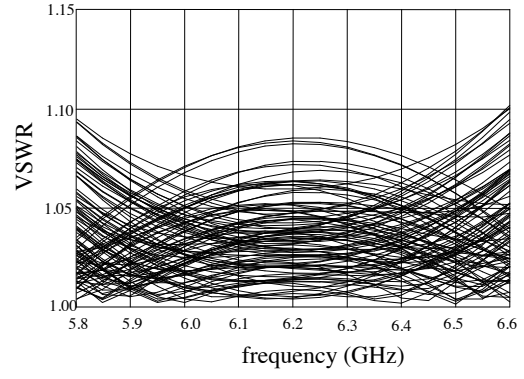


(b)

Fig. 3. Statistical analysis for the two-section waveguide transformer assuming uniform distribution with relative tolerances of 1.0%, (a) using the SDMM, and (b) using fine model simulations.

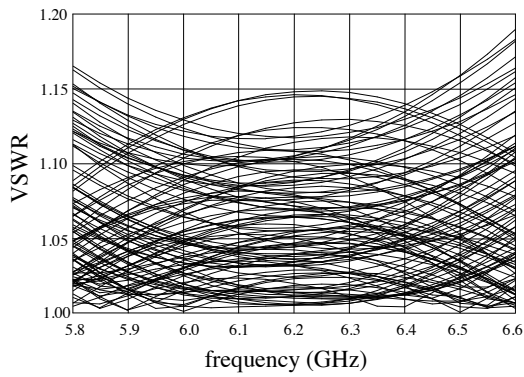


(a)

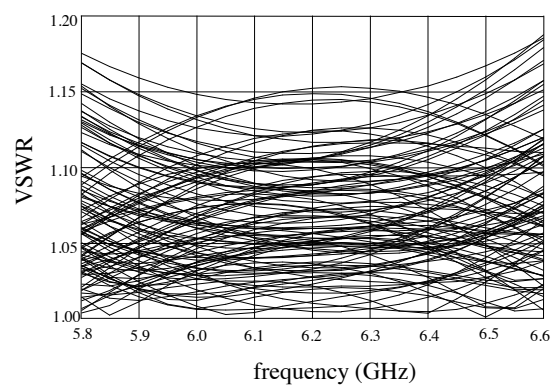


(b)

Fig. 4. Statistical analysis for the two-section waveguide transformer assuming uniform distribution with relative tolerances of 2.0%, (a) using the SDMM, and (b) using fine model simulations.



(a)



(b)

Fig. 5. Statistical analysis for the two-section waveguide transformer assuming uniform distribution with relative tolerances of 4.0%, (a) using the SDMM, and (b) using fine model simulations.

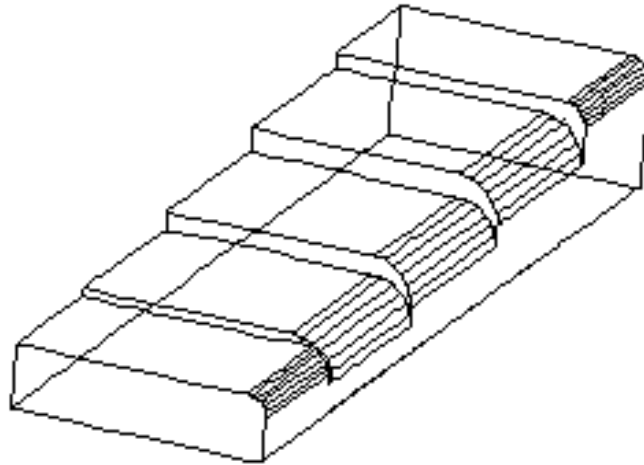


Fig. 6. The simulated part of the three-section waveguide transformer with rounded corners [6].

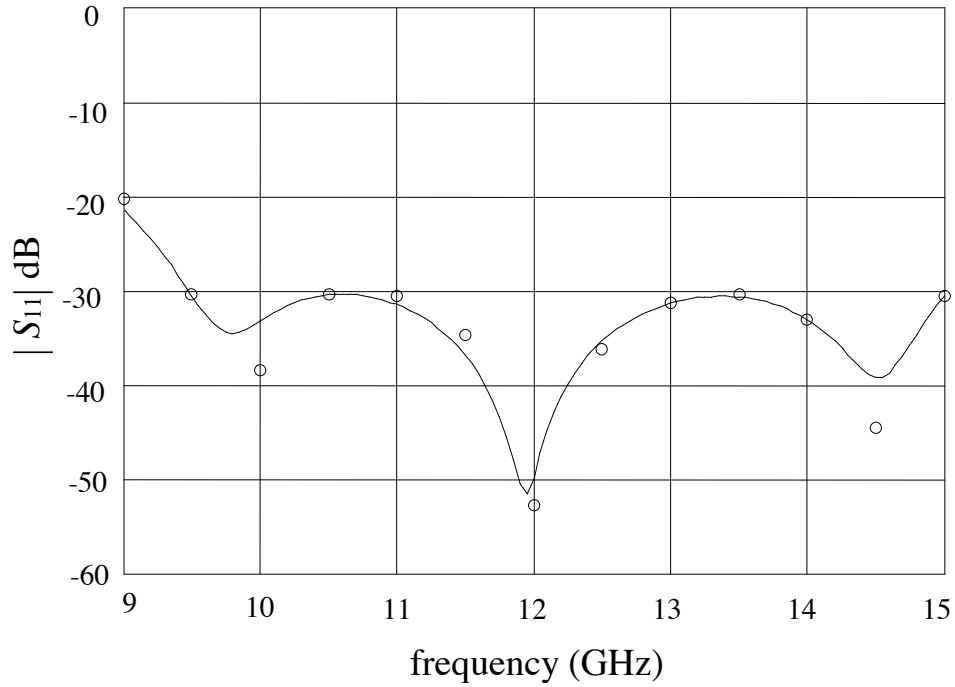
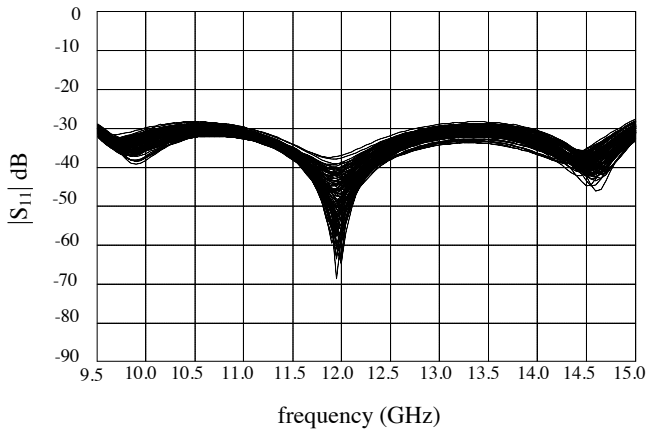
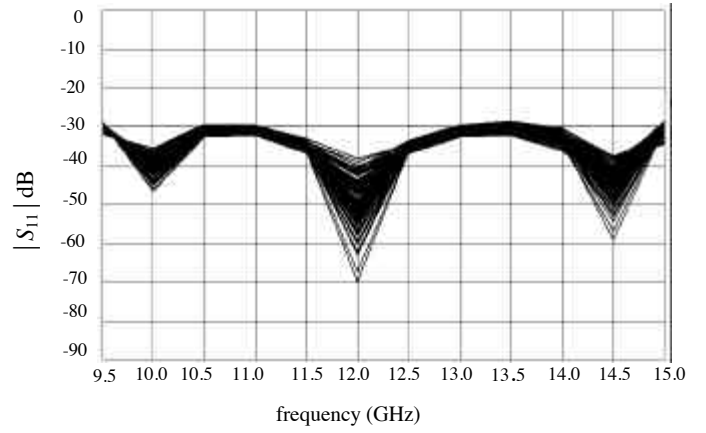


Fig. 7. The optimal fine model response (o) and the response (—) at the corresponding coarse model point for the three-section waveguide transformer with rounded corners.

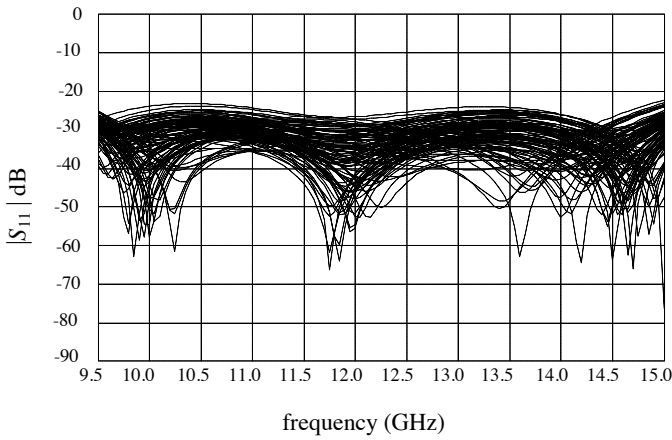


(a)

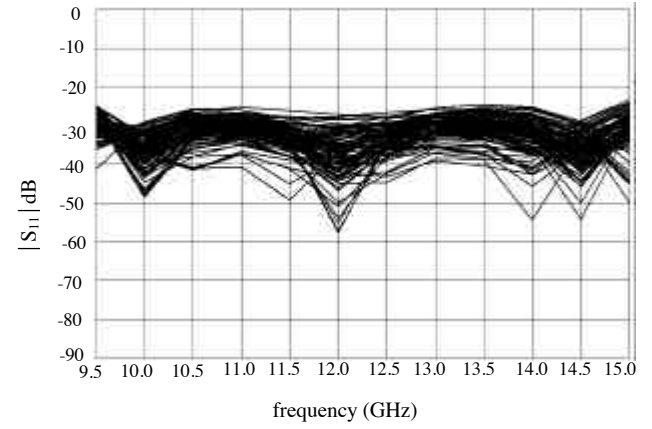


(b)

Fig. 8. Statistical analysis for the three-section waveguide transformer assuming uniform distribution with relative tolerances of 0.5%, (a) using the SDMM, and (b) using fine model simulations.

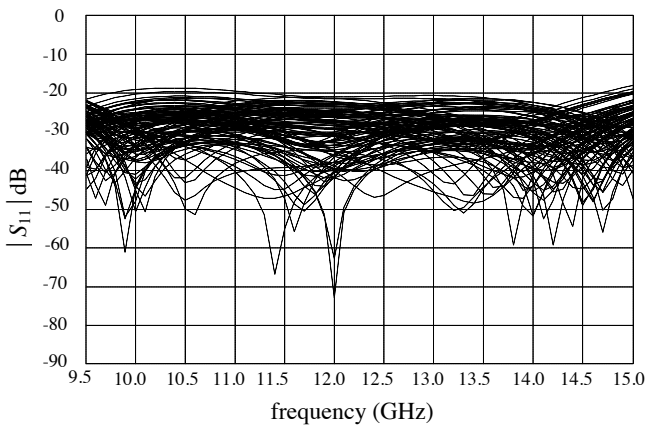


(a)

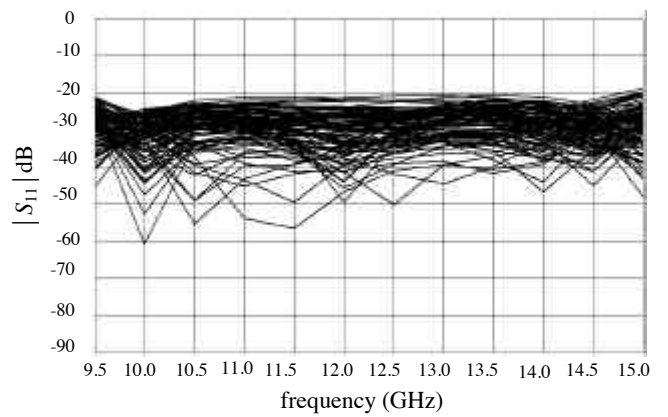


(b)

Fig. 9. Statistical analysis for the three-section waveguide transformer assuming uniform distribution with relative tolerances of 2%, (a) using the SDMM, and (b) using fine model simulations.



(a)



(b)

Fig. 10. Statistical analysis for the three-section waveguide transformer assuming uniform distribution with relative tolerances of 4%, (a) using the SDMM, and (b) using fine model simulations.

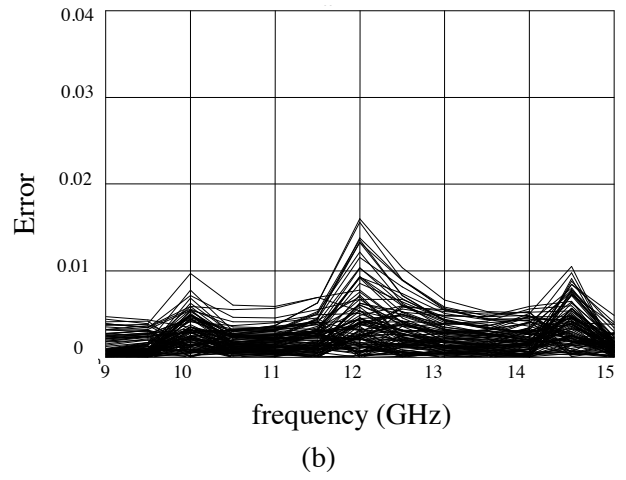
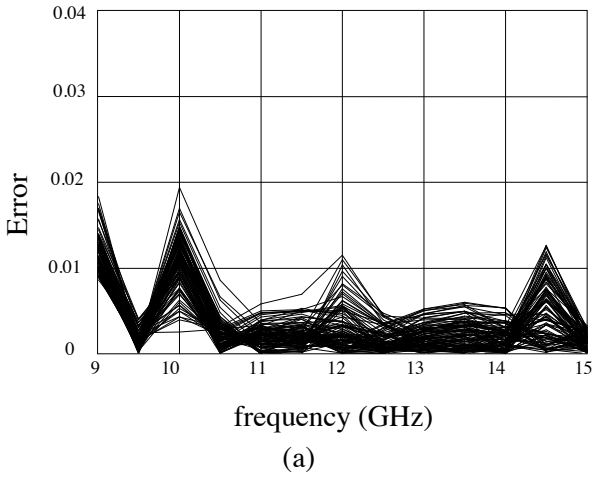


Fig. 11. Error in the statistical analysis for the three-section waveguide transformer assuming uniform distribution with relative tolerances of 0.5%, (a) using SDMM, and (b) using linear approximation.

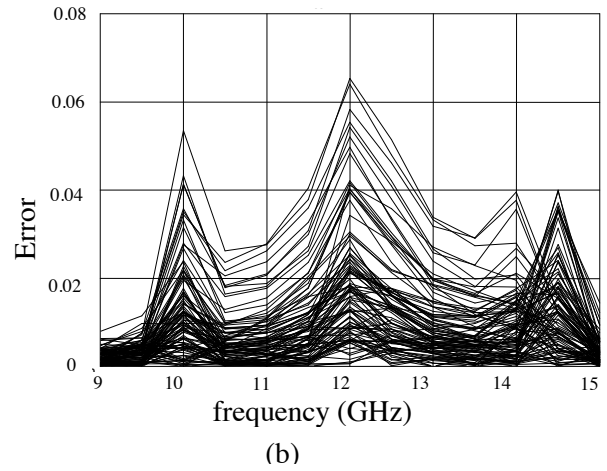
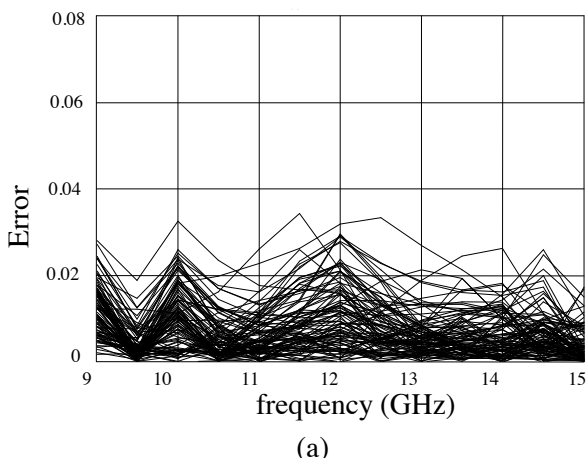


Fig. 12. Error in the statistical analysis for the three-section waveguide transformer assuming uniform distribution with relative tolerances of 2%, (a) using SDMM, and (b) using linear approximation.

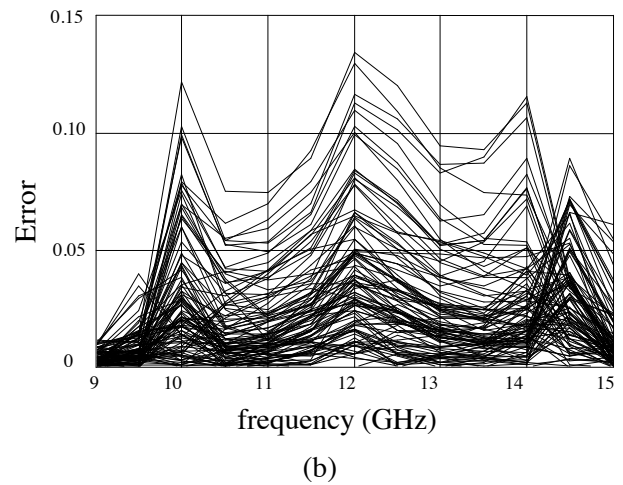
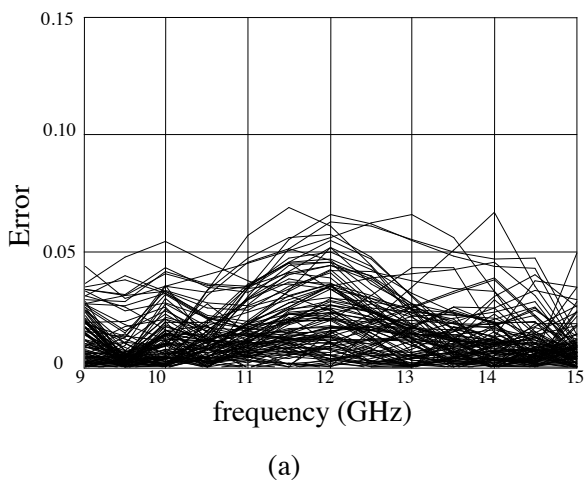


Fig. 13. Error in the statistical analysis for the three-section waveguide transformer assuming uniform distribution with relative tolerances of 4%, (a) using SDMM, and (b) using linear approximation.

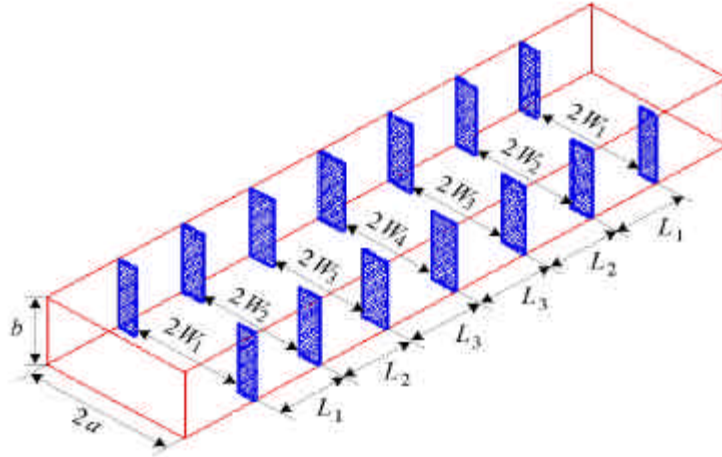


Fig. 14. The fine model of the six-section waveguide filter [11, 12].

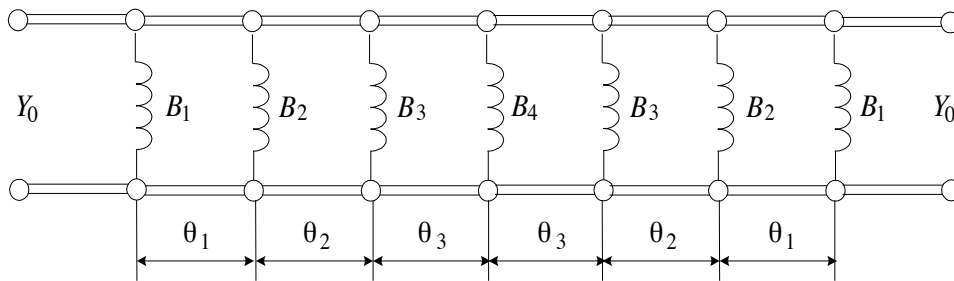


Fig. 15. The coarse model of the six-section waveguide filter [13].

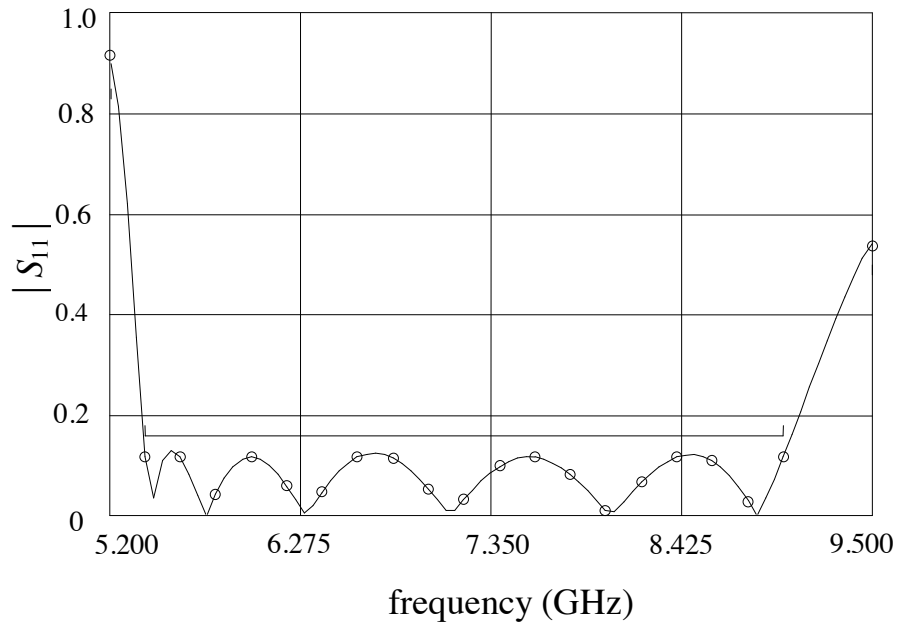


Fig. 16. The fine model response (o) and the response (—) at the extracted coarse model point for the six-section waveguide filter.

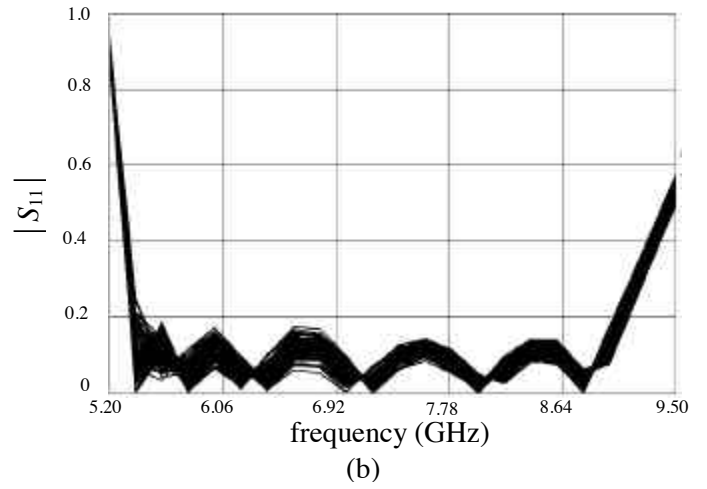
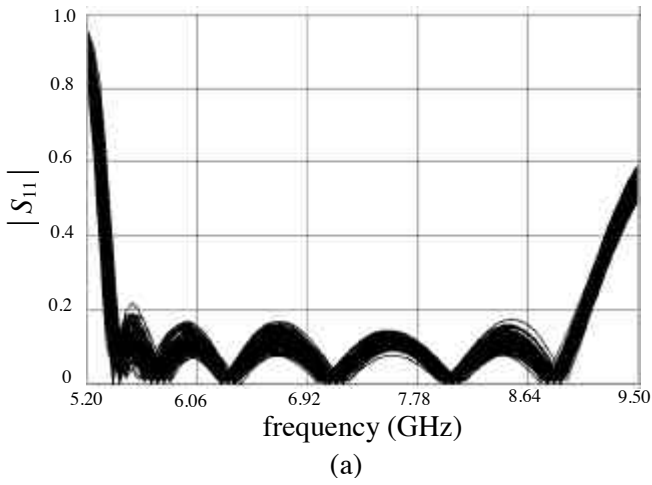


Fig. 17. Statistical analysis for the six-section waveguide filter assuming uniform distribution with relative tolerances of 1%, (a) using the SDMM, and (b) using fine model simulations.

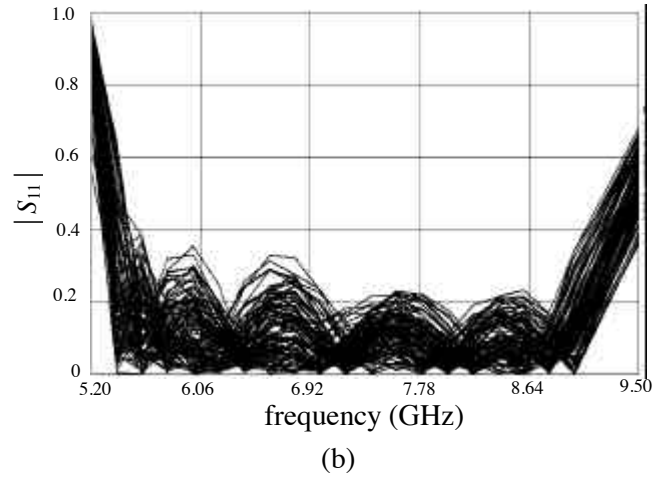
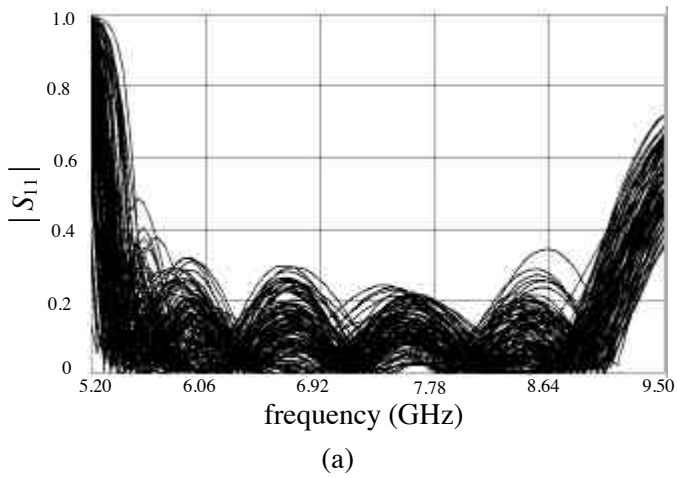


Fig. 18. Statistical analysis for the six-section waveguide filter assuming uniform distribution with relative tolerances of 4%, (a) using the SDMM, and (b) using fine model simulations.

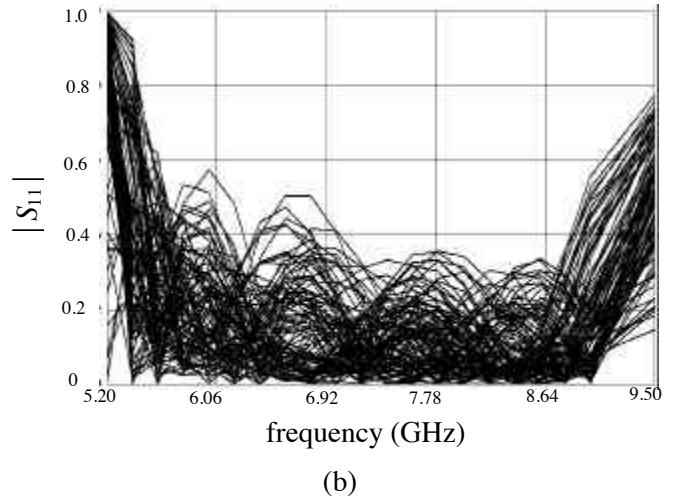
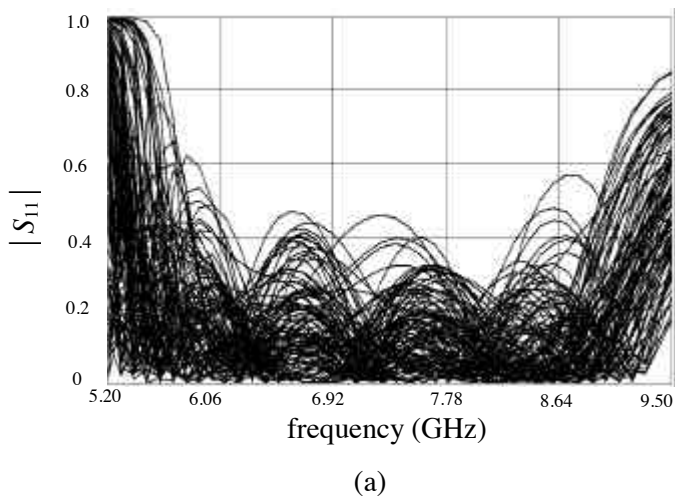


Fig. 19. Statistical analysis for the six-section waveguide filter assuming uniform distribution with relative tolerances of 8%, (a) using the SDMM, and (b) using fine model simulations.

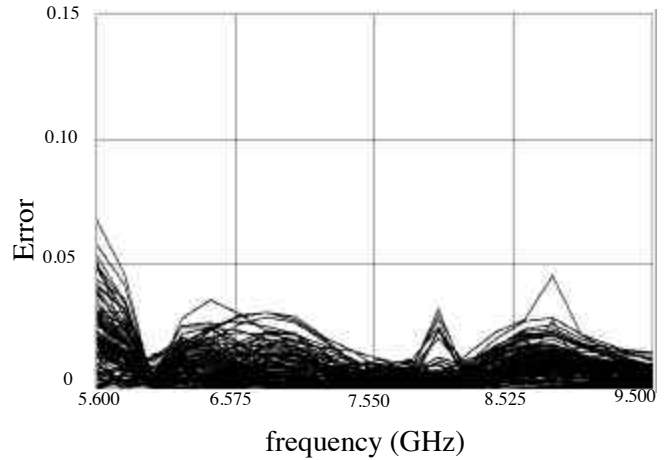
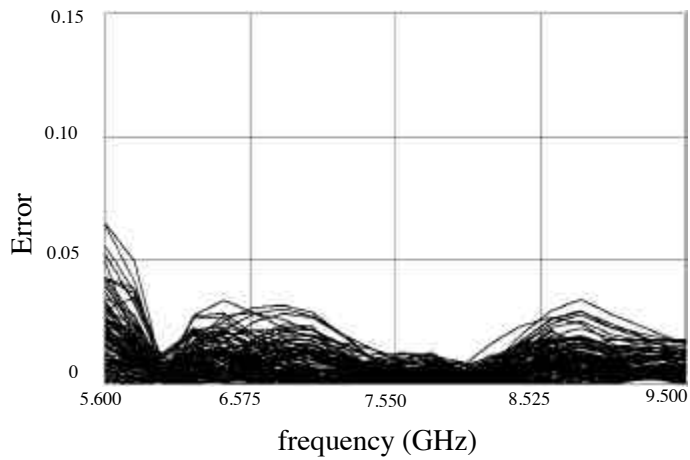


Fig. 20. Error in the statistical analysis for the six-section waveguide filter assuming uniform distribution with relative tolerances of 1%, (a) using SDMM, and (b) using linear approximation.

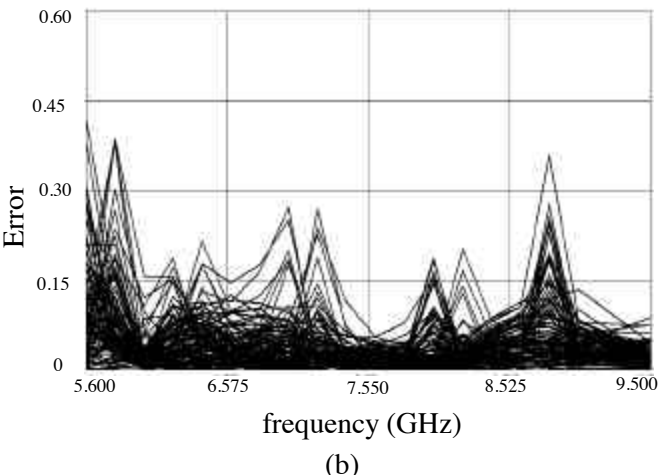
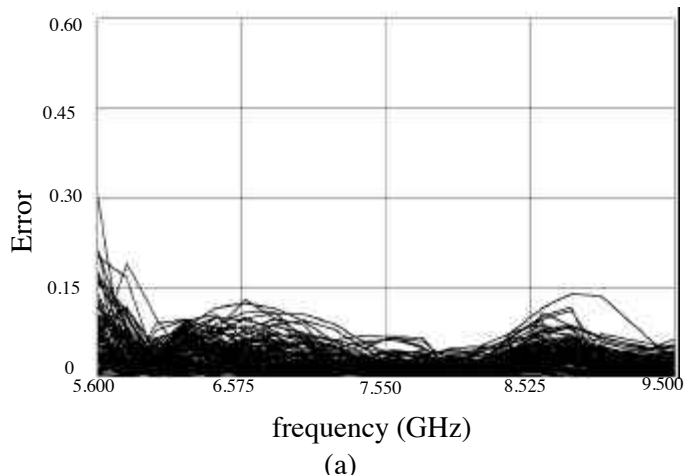


Fig. 21. Error in the statistical analysis for the six-section waveguide filter assuming uniform distribution with relative tolerances of 4%, (a) using SDMM, and (b) using linear approximation.

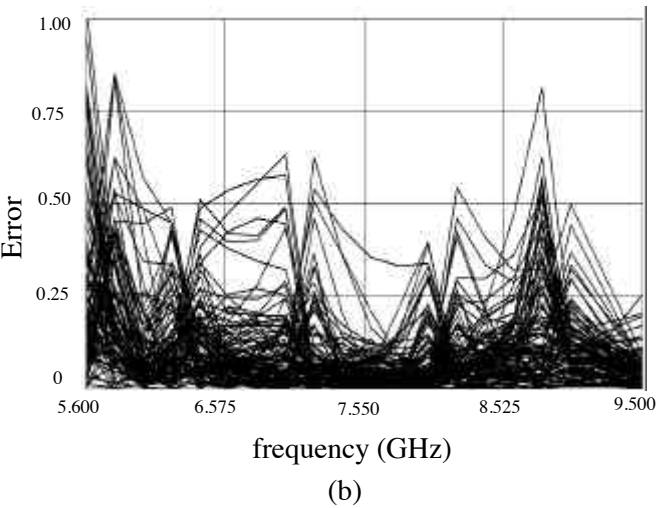
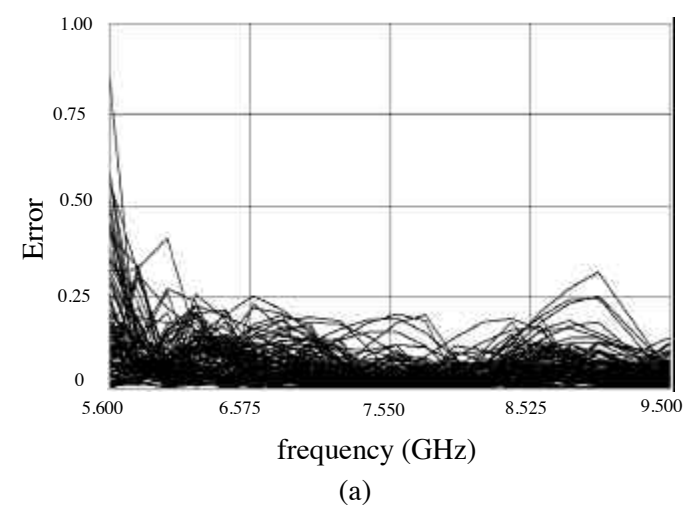


Fig. 22. Error in the statistical analysis for the six-section waveguide filter assuming uniform distribution with relative tolerances of 8%, (a) using SDMM, and (b) using linear approximation.

